Robust Nonlinear Control of BLDC Motor in Quadcopter Applications

Steven T. Elliott and Thomas W. Carr

Department of Mathematics, Southern Methodist University, Dallas, TX

Student: stelliott@smu.edu
Mentor: tcarr@smu.edu

ABSTRACT
This paper describes the development of a nonlinear closed loop motor control system for a quadcopter micro-unmanned aerial vehicle (micro-UAV) platform. Research groups have analyzed the performance of brushless direct current (BLDC) motors with nonlinear effects in various applications, focusing on areas such as friction's effect on position. This paper analyzes the nonlinear effects of BLDC motors on speed when these motors are used in quadcopter flying robots. Notably, to account for nonlinear torque from the aerodynamic forces on a quadcopter rotor, a Control Lyapunov Function (CLF) approach is used in designing a stable feedback control system. The paper also explains the custom model and simulation of the system built in MATLAB/Simulink used to demonstrate and quantify the successful performance of the design.

KEYWORDS
Control Lyapunov Function; Micro-Unmanned Aerial Vehicle; Aerial Robotics; Quadcopters; Nonlinear Motor Control

INTRODUCTION

One area of research and development that has enormous potential is the multicopter micro-UAV. This flying robot typically uses four propellers, one mounted on each of the four ends of a cross-shaped frame as shown in **Figure 1**. Two propellers lying opposite to each other both rotate clockwise, and the other pair rotates counterclockwise, canceling the torques. Pitch, roll, and yaw movements are achieved by varying the speed of the motors; the robot carries an onboard controller and battery as well.[1] Quadcopters range in size as small as 6 centimeters from tip to tip and 3 grams in weight.[2]

Figure 1. A quadcopter micro-UAV.

With their vertical flight and hover abilities, durability, and ease of use both indoors and outdoors, quadcopters are growing in popularity and have many promising applications, either as individual vehicles or in cooperation with others.[2–5] Some of the uses include search and rescue, surveillance, exploration, photography, transport, and construction; quadcopters can be particularly helpful in environments that are inaccessible, contaminated, or otherwise dangerous.[6, 7]

The performance of the quadcopter depends on the speed of response of the motors in achieving controlled, stable flight. Research groups studying quadcopters often assume unchanging aerodynamics, but quadcopters experience significant aerodynamic disturbance effects due to their surroundings, complex interactions with multiple UAVs or, at small scales, even to mild wind gusts.[7, 8] Researchers often deal with these by reducing the speed, keeping greater distance between the quadcopter and its surroundings, using simpler trajectories, attempting to limit the roll and pitch angles, and controlling the environment.[2]

Quadcopters are poised to become a widely used technology, and improvements in quadcopter controls could have a significant impact on their efficacy. Researchers have taken many different approaches to this control system design, summarized well in **References 6, 7, 9**. A few of the techniques include vehicle control loops that use feedback linearization for velocity and attitude control,[1, 4] proportional-integral-derivative (PID) control for attitude and position,[2, 5] a predictor-corrector algorithm for angular velocity control,[4] sequences of controllable trajectories accomplishing more complex maneuvers,[5] iterative learning,[5] and a decentralized adaptive controller for attitude and altitude.[9] Instead, this work focuses on a fundamental control problem for quadcopter systems: the stable and precise response of the onboard low-level motor controllers.

Quadcopters use Brushless DC (BLDC) motors, each with an electronic controller that determines the rotor's phase over time (and therefore speed) via a sensor or with so-called sensorless methods, and uses the information to drive the rotor's rotation. BLDCs offer advantages over the older, electromechanically commutated, brushed DC motors: greater power efficiency, finely-adjustable speed, precise motion control, ease of programmability, and low maintenance.[10]

Other research groups have analyzed the performance with nonlinear effects of BLDCs in various applications, focusing on areas such as the effect of friction on position.[11, 12] In particular, this paper differs from the work done by Sabra *et al.*[11] since this paper analyzes the nonlinear effects of BLDC motors on speed for quadcopter applications, and this paper utilizes a set point tracking analysis to ensure that the system is stable around a constant equilibrium point. Specifically, the goal of this work is to derive a nonlinear closed loop feedback control equation and prove the stability of the system using Lyapunov stability analysis with a Control Lyapunov Function (CLF). This work includes a simulation in MATLAB/Simulink of a propeller/BLDC motor system with friction, propeller torque and damping control. The simulation implements the model system and is used to demonstrate and measure the performance of the system.

This paper is organized as follows. The *Methods and Procedures* section contains subdivisions explaining CLF theory, the quadcopter motor model, Lyapunov analysis, and the custom Simulink simulation. The *Results and Discussion* section is next, followed by the final section which offers conclusions and areas for further research.

METHODS AND PROCEDURES

Theory of CLF

This project builds on prior research using CLF as a method of controlling nonlinear systems.[1, 11, 13] Lyapunov stability, developed by mathematician Aleksandr Mikhailovich Lyapunov, guarantees the stability of a closed nonlinear system when certain scalar functions, the Lyapunov functions, meet a set of criteria summarized below.

Consider a nonlinear system represented by the following state space equation:

$$\dot{x} = F(x,u);\ x \in \mathbb{R}^n\ ; u \in \mathbb{R}^m. \qquad \textbf{Equation 1.}$$

F is a vector field in $\mathbb{R}^n$, x represents the state variables, and u represents the control function.

A Lyapunov function, denoted $V(x)$, must fulfill certain requirements to prove system stability. $V(x)$ is positive definite if $V(0) = 0$ and $V(x) > 0$ for $x \neq 0$, while the time derivative $\dot{V}(x)$ is negative definite if $\dot{V}(0) = 0$ and $\dot{V}(x) < 0$ for $x \neq 0$. If $V(x)$ is a continuously differentiable positive definite function such that $\dot{V}(x)$ is negative definite, then the system is asymptotically stable; if no suitable Lyapunov equations can be found such that $V(x)$ and $\dot{V}(x)$ are not positive definite and negative definite, respectively, then the system cannot be proven to be asymptotically stable.[14, 15]

While the Lyapunov functions for some nonlinear systems are physical energy functions, in many cases there is no specific method for crafting Lyapunov functions, which then must be found through trial and error.

A nonlinear system is considered affine (or linear-in-control, since a linear proportional controller is used to control the nonlinear system) with respect to the input when the system has the form

$$\dot{x} = F(x,u) = f_0(x) + \sum_{i=1}^{m} u_i f_i(x)\,. \qquad \textbf{Equation 2.}$$

Since $x \in \mathbb{R}^n$, the $f_i, i = 0, 1, \dots, m$, are vector fields in $\mathbb{R}^n$. Specifically, they are $j = 1, 2, \dots, n$ equations of the form

$$\dot{x}_j = f_{0j}(x) + \sum_{i=1}^{m} u_i f_{ij}(x)\,. \qquad \textbf{Equation 3.}$$

The system is assumed to have an initial condition $x = 0$ such that $F(0, u) = 0$. Assume a positive definite Control Lyapunov Function, $V(x)$, exists where x represents all variables implemented in the Lyapunov function. Therefore,

$$\dot{V}(x) = \nabla V \cdot \frac{dx}{dt} = \sum_{j=1}^{n} \frac{\partial V}{\partial x_j}\frac{dx}{dt}\,. \qquad \textbf{Equation 4.}$$

Substituting for $\dot{x}$ gives

$$\begin{aligned} \dot{V} &= \nabla V \cdot \left(f_0 + \sum_{i=1}^{m} u_i f_i \right), \\ &= \nabla V \cdot f_0 + \sum_{i=1}^{m} u_i (\nabla V \cdot f_i)\,. \end{aligned} \qquad \textbf{Equation 5.}$$

If $u_i = -\nabla V \cdot f_i$, then

$$\dot{V} = \nabla V \cdot f_0 - \sum_{i=1}^{m} (\nabla V \cdot f_i)^2. \qquad \textbf{Equation 6.}$$

This feedback law, $u_i = -\nabla V \cdot f_i$, is called damping control.[14]

The Quadcopter Motor Model

The damping control method explained above will now be applied to the system depicted in **Figure 2**. The system is an equivalent circuit model containing a control voltage, a characteristic resistance and inductance, and a DC motor driving a propeller.

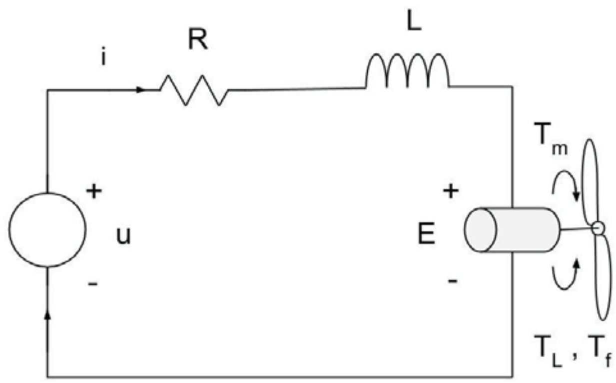

Figure 2. An equivalent circuit model of a series DC motor.

Table 1 shows the motor parameters used in the model. In addition to the common features of a typical motor such as resistance, inductance, current, angular velocity, and moment of inertia, several other parameters are included in order to model nonlinearities effectively. For example, the model includes back EMF, which is induced when the permanent magnets in the motor rotate. Also included is the torque constant, which represents the torque generated by the current flowing through the motor. The viscous friction coefficient represents the friction generated by the rotating motor shaft, and the propeller aerodynamic constant is a measure of how the form of the propeller generates torque on the motor shaft as it rotates and creates thrust in air of a given density.

Parameter	Description	Units
u_1	Control voltage	Volts, V
L	Inductance	Henrys, H
I	Motor current	Amperes, A
R	Resistance	Ohms, Ω
K_e	Back EMF constant	V s / rad
v_0	Input voltage	Volts, V
ω	Rotor angular velocity	rad / s
J	Moment of inertia	kg m^2
K_t	Torque constant	N m / A
b	Viscous friction coefficient	N m s / rad
K_A	Propeller aerodynamic constant	kg m^2 N^2 / s^2

Table 1. Parameters for the motor model.

The model of the dynamic BLDC motor driving a propeller is represented by a set of nonlinear state equations. The equation for ω includes the nonlinear term $K_A\,|\omega|\omega$, which represents the magnitude and direction of the propeller torque:

$$\dot{I} = \frac{1}{L}(-RI - K_e\omega + v_0), \text{ and}$$
$$\dot{\omega} = \frac{1}{J}(-b\omega + K_tI - K_A\omega|\omega|). \qquad \textbf{Equation 7.}$$

Alternatively:

$$\dot{\omega} = \frac{1}{J}(-b\omega + K_tI - K_A\omega^2) \text{ for } \omega > 0.$$
$$\dot{\omega} = \frac{1}{J}(-b\omega + K_tI + K_A\omega^2) \text{ for } \omega < 0. \qquad \textbf{Equation 8.}$$

First, an analysis of the motor model with a fixed set point — or target state that the control system seeks to maintain — is developed. The equations relating change in current and change in angular velocity around the set point are given by

$$\Delta I + I_0 = I \text{ and } \Delta\omega + \omega_0 = \omega, \qquad \textbf{Equation 9.}$$

where I_0 and ω_0 represent a non-zero equilibrium point resulting from a constant input voltage, v_0. Specifically, they satisfy

$$0 = \frac{1}{L}(-RI_0 - K_e\omega_0 + v_0) \text{ and } 0 = \frac{1}{J}(-b\omega_0 + K_tI_0 - K_A\omega_0^2)\,.$$

To ensure that the system can track a constant set point, the expressions for I and ω are substituted into the state equations for change in current and change in angular velocity as follows, starting with the equation for current:

$$\dot{I} = \frac{1}{L}(-R\Delta I - RI_0 - K_e\Delta\omega - K_e\omega_0 + v_0)\,. \qquad \textbf{Equation 10.}$$

Substituting for I_0 and ω_0, another expression is obtained,

$$\dot{I} = \frac{1}{L}(-R\Delta I - K_e\Delta\omega), \quad \textbf{Equation 11.}$$

which is similar in form to the original state equation. Next, the set point analysis for the change in angular speed is developed. For the case $\omega > 0$ and after substituting for I_0 and ω_0,

$$\dot{\omega} = \frac{1}{J}(-(b + 2K_A\omega_0)\Delta\omega + K_t\Delta I - K_A\Delta\omega^2)\,. \quad \textbf{Equation 12.}$$

The above analysis transforms the state equations to be dependent on variables ΔI and $\Delta\omega$, or the distance moved in current and angular velocity from the equilibrium point I_0 and ω_0. Next, a Lyapunov analysis will be conducted on the new state equations to demonstrate that the system is globally asymptotically stable around that equilibrium point.

Lyapunov Analysis

Let the chosen Control Lyapunov Function V be a function of two variables ΔI and $\Delta\omega$ with c_1 and c_2 being control parameters:

$$V = \frac{1}{2}c_1\Delta I^2 + \frac{1}{2}c_2\Delta\omega^2\,. \quad \textbf{Equation 13.}$$

Since $V > 0$ for all values of $\Delta I \neq 0$ and $\Delta\omega \neq 0$, and $V = 0$ when $\Delta I = \Delta\omega = 0$, V is a positive definite function, which meets the first Lyapunov requirement. $\dot{V}$ is given by the equation (for $\Delta\omega > 0$):

$$\begin{aligned} \dot{V} &= c_1\Delta I\Delta\dot{I} + c_2\Delta\omega\Delta\dot{\omega} \\ &= -\frac{c_1R\Delta I^2}{L} - \frac{c_1K_e\Delta I\Delta\omega}{L} - \frac{c_2(b + 2K_A\omega_0)\Delta\omega^2}{J} + \frac{c_2K_t\Delta I\Delta\omega}{J} - \frac{c_2K_A\Delta\omega^3}{J}\,. \end{aligned} \quad \textbf{Equation 14.}$$

For $\omega < 0$, the above equation is replaced with the following:

$$\dot{V} = -\frac{c_1R\Delta I^2}{L} - \frac{c_1K_e\Delta I\Delta\omega}{L} - \frac{c_2(b + 2K_A\omega_0)\Delta\omega^2}{J} + \frac{c_2K_t\Delta I\Delta\omega}{J} + \frac{c_2K_A\Delta\omega^3}{J}\,. \quad \textbf{Equation 15.}$$

In both cases, $\dot{V} = 0$ when $\Delta I = \Delta\omega = 0$. To ensure that $\dot{V}$ is negative definite and $\dot{V} < 0$ for all values of $\Delta I \neq 0$ and $\Delta\omega \neq 0$, $-\frac{c_1K_e\Delta I\Delta\omega}{L}$ and $\frac{c_2K_t\Delta I\Delta\omega}{J}$ must cancel to zero. For this to occur, $\frac{c_1K_e\Delta I\Delta\omega}{L} = \frac{c_2K_t\Delta I\Delta\omega}{J}$ and $\frac{c_1}{c_2} = \frac{K_tL}{K_eJ}$. Therefore, as long as $\frac{c_1}{c_2} = \frac{K_tL}{K_eJ}$, $\dot{V}$ is negative definite, which meets the second Lyapunov requirement, and thus the system is asymptotically stable.

Next, the damping control analysis is carried out by casting the equations back into the form of **Equation 3**, with $n = 2$ and $m = 1$, mapping $[x_1 \quad x_2] = [\Delta I \quad \Delta\omega]$.

$$\begin{bmatrix}\dot{x}_1 \\ \dot{x}_2\end{bmatrix} = \begin{bmatrix} -\frac{R}{L}x_1 - \frac{K_e}{L}x_2 \\ \frac{K_t}{J}x_1 - \frac{b+2K_A\omega_0}{J}x_2 - \frac{K_A}{J}x_2^2 \end{bmatrix} + u_1\begin{bmatrix}\frac{1}{L} \\ 0\end{bmatrix} \quad \textbf{Equation 16.}$$

$$\nabla V(x) = [c_1\Delta I \quad c_2\Delta\omega] \quad \textbf{Equation 17.}$$

Substituting **Equations 6** and **9** results in a new damping control function.

$$u_1 = \frac{-c_1\Delta I}{L} \quad \textbf{Equation 18.}$$

Simulation
The simulation of the electrical current control of the DC motor was created in MATLAB/Simulink, and the block diagram is shown below. The block diagram implements the two state equations and damping control function that were explained previously. The design uses standard components like the integrator, gain, adder, and multiplier blocks, as well as the user-selected parameters that define system dynamics. Simulink calculates the system response to the user's inputs and initial conditions, and displays are the user-selected data signals, while dynamically showing rise time, settling time, and more.

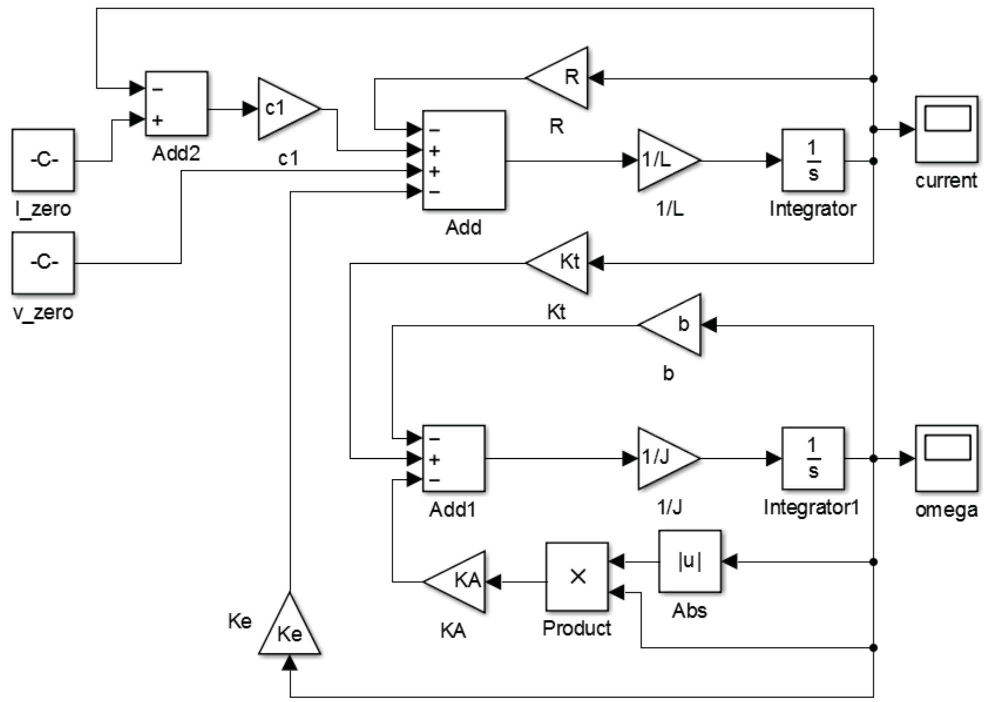

Figure 3. Simulink model of the electric current control for the DC motor.

The constant I_0 input, similar to a current setpoint in a control system, complements the effects of the setpoint voltage, v_0, and speeds up the response of the system. The net constant input to the system is $v_0 + c_1 I_0$.

The baseline motor parameter values in **Table 2** below, except for K_A, were taken from the datasheet of a well characterized, commercially available, BLDC motor that possesses a power specification typical of quadcopter motors.[16] The value of K_A was calculated from a static coefficient taken from publicly available quadcopter research data.[17] Specifically, the propeller coefficient for a 10×5 inch propeller, $C_P = 0.04$, was substituted into the equation:

$$K_A = \frac{C_P \rho_{air} D}{2\pi} \qquad \textbf{Equation 19.}$$

where $\rho_{air} = 1.225$ kg/m^3 and D, which equals 0.254 m (10 inches), is the diameter of a typical quadcopter rotor, resulting in a K_A of 8.24×10^{-6} kg m^2 N^2/s^2.

Parameter	Baseline value
L	0.48 mH
I	Motor current, A
R	0.70 Ω
K_e	$1.10 \cdot 10^{-2}$ V s / rad
ω	Rotor angular velocity, rad / s
J	$3.60 \cdot 10^{-6}$ kg m^2
K_t	0.0109 N m / A
b	$3.30 \cdot 10^{-4}$ N m s / rad
K_A	$8.24 \cdot 10^{-6}$ kg m^2 N^2 / s^2

Table 2. Baseline motor parameter values.

RESULTS AND DISCUSSION

According to the Lyapunov stability analysis demonstrated earlier, the motor control system simulated in Simulink should be able to track a constant set point while remaining asymptotically stable. As a demonstration, the simulation was run with various values for control parameter c_1 and using the baseline parameters in **Table 2**. A graph of current versus time for various values of c_1 is shown in **Figure 4** below, and a graph of angular velocity versus time for various values of c_1 is shown in **Figure 5** below. The system showed stable behavior since it could track rise times smoothly for all values of c_1 tested, with rise time being the time elapsed during the transition from 10% to 90% of its steady state current or angular velocity, starting from zero. Note that the system tracked rise times smoothly and quickly, with no overshoot, oscillation, or other signs of instability.

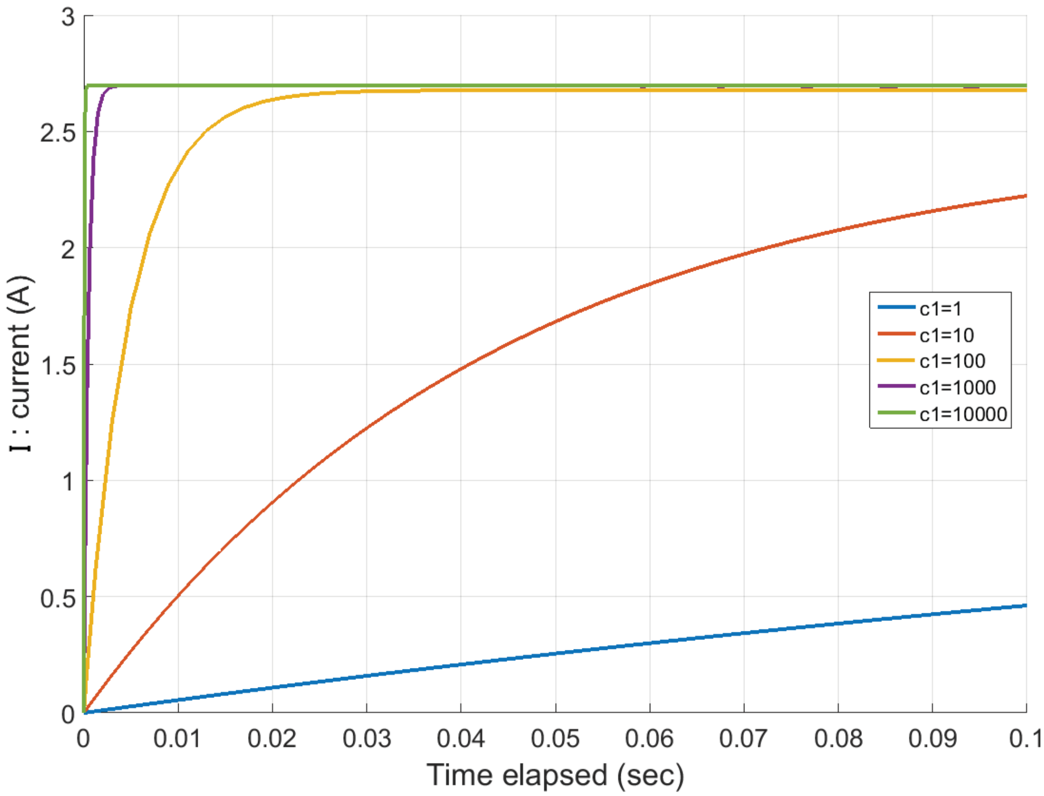

Figure 4. Simulation current response for a range of control parameter c_1, but motor parameters held constant.

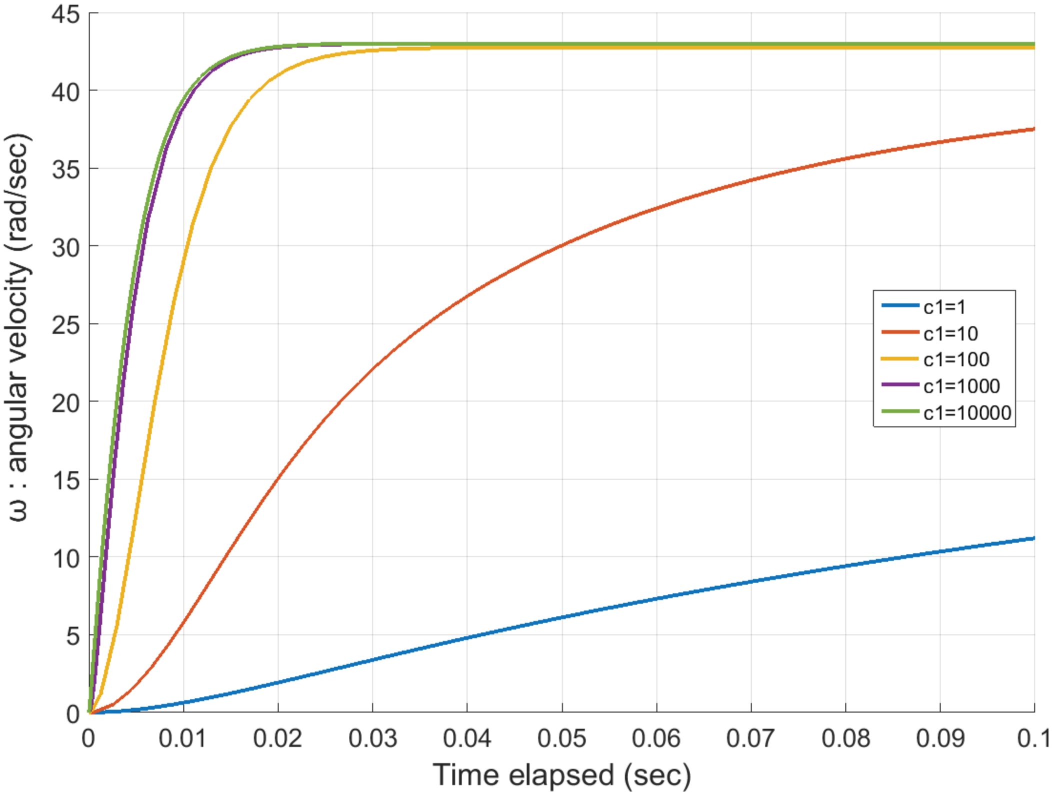

Figure 5. Simulation angular velocity response for a range of control parameter c_1, but motor parameters held constant.

As these results demonstrate, the larger c_1 values result in faster response times, while the system remains stable even for very high values of c_1, consistent with theory. However, to further demonstrate the robustness of the system, another test must be completed. In the next test, the values of physical parameters are decreased or increased to examine the effect on system performance.

The parameters that vary during this test are $R, L, K_e, b, J, K_t,$ and K_A. In the real world, the physical parameters that determine the performance of the quadcopter BLDC may vary from nominal values due to measurement errors, manufacturing variance, and environment changes such as temperature and air density. **Figure 6** below shows the simulated steady state current as c_1 increases with varying motor parameter values. To illustrate a wide variation from nominal, all the parameters are inputted as either 50% or 200% of the baseline values. Simulations test all parameters set at both percentages and for all possible combinations. The graph in **Figure 6** below shows that the steady-state current value is robust to variations in all motor parameters tested. Steady-state current variation in the presence of motor parameter variation improves a great deal as the control parameter c_1 increases. These results demonstrate that the system is robust to variations in motor parameter values, since the system remains stable for the wide variation of parameter values tested and the response varies in a narrow range.

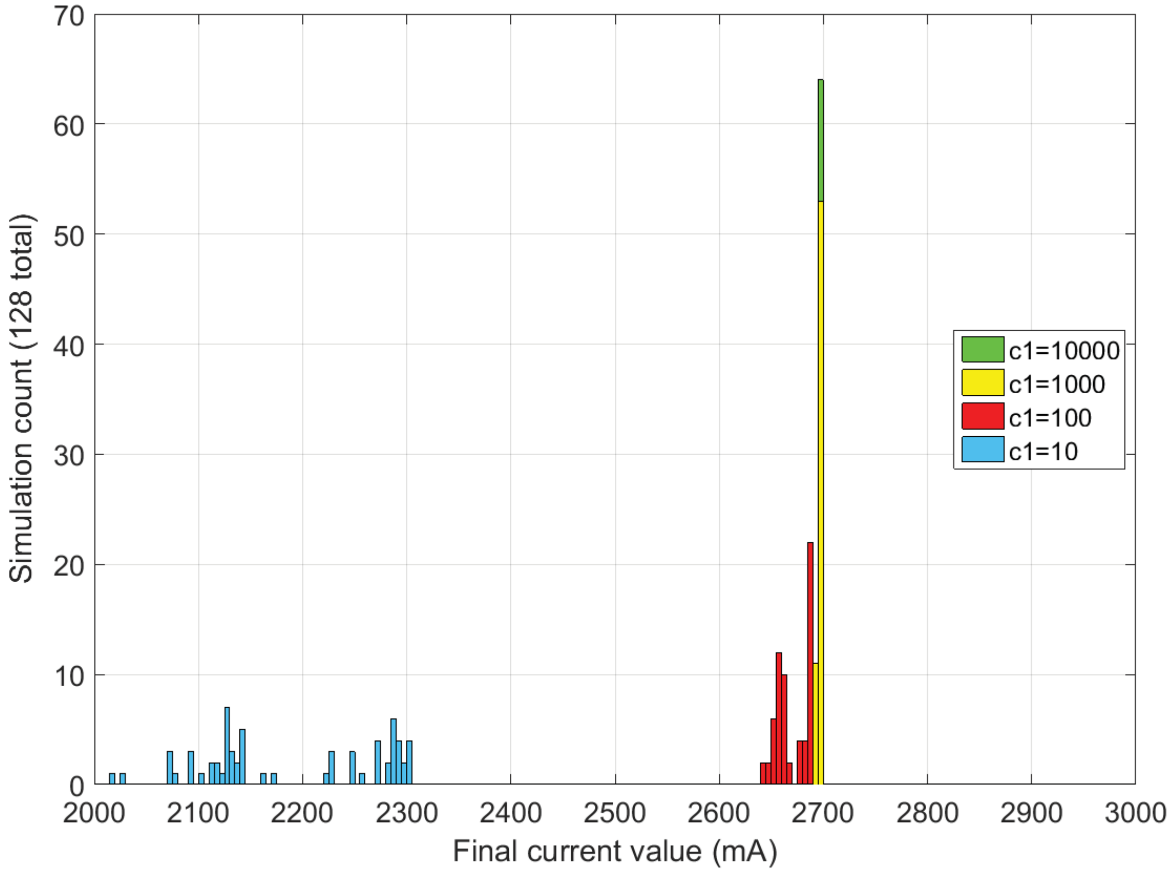

Figure 6. Histograms showing steady-state current variation across all motor parameter combinations. As c_1 increases, the variation improves to near zero at $c_1 = 10000$.

CONCLUSIONS

As shown, Lyapunov stability theory was applied to closed loop current control of a BLDC motor. A Lyapunov function was designed with associated feedback control that was proven to make the system stable. A model and simulation of the nonlinear BLDC motor showed the accuracy and robustness of the mathematical derivation.

There are several potential paths for future research on this motor control system. One topic for future research could be to include a full PID controller to minimize steady state error and possibly improve response time, and analyze the PID controller for stability. In addition, considering that the damping control method resulted in feedback only for the electric current variable, another area of study could be to use a different analysis technique that allows feedback control using the speed variable, including possibly a PID controller for speed. A third area for future research could be to build a physical model of the system and compare this model to the theory behind it.

REFERENCES

1. Voos, H. (2009) Nonlinear control of a quadrotor micro-UAV using feedback-linearization, in *Proceedings 2009 IEEE International Conference on Mechatronics*, Malaga, Spain.

2. Michael, N., Mellinger, D., Lindsey, Q., and Kumar, V. (2010) The GRASP multiple micro-UAV testbed, in *IEEE Robotics and Automation Magazine* 17(3), 56–65.

3. Gurdan, D., Stumpf, J., Achtelik, M., Doth, K., Hirzinger, G., and Rus, D. (2007) Energy-efficient autonomous four-rotor flying robot controlled at 1 kHz, in *Proceedings 2007 IEEE International Conference on Robotics and Automation*, Roma, Italy.

4. Lupashin, S., Hehn, M., Mueller, M. W., Schoellig, A. P., Sherback, M., and D'Andrea, R. (2014) A platform for aerial robotics research and demonstration: the Flying Machine Arena, *Mechatronics* 24(1), 41–54.

5. Mellinger, D., Michael, N., and Kumar, V. (2012) Trajectory generation and control for precise aggressive maneuvers with quadrotors, *International Journal of Robotics Research* 31(5), 664–674.

6. Dong, W., Gu, G., Zhu, X., and Ding, H. (2015) Development of a quadrotor test bed — modeling, parameter identification, controller design and trajectory generation, *International Journal of Advanced Robotic Systems*, 1–14.

7. Hoffmann, G., Huang, H., Waslander, S., and Tomlin, C. (2007) Quadrotor helicopter flight dynamics and control: Theory and experiment, in *AIAA Guidance, Navigation and Control Conference and Exhibit*, Hilton Head, South Carolina.

8. Belatti, T., Kumar, V., Powers, C. University of Pennsylvania School of Engineering and Applied Science SUNFEST Program, Quadrotor flight in constrained environments, http://www.seas.upenn.edu/sunfest/docs/papers/12-belatti.pdf (accessed June 2015)

9. Mohammadi, M., and Shahri, A. (2013) Adaptive nonlinear stabilization control for a quadrotor UAV: Theory, simulation, and experimentation, *Journal of Intelligent and Robotic Systems*, 105-122.

10. Hughes, A., and Drury, D. (2013) *Electric Motors and Drives: Fundamentals, Types and Applications* 3rd ed., 357–358, Newnes, Oxford, UK.

11. Sabra, M., Khasawneh, B., and Zohdy, M. (2014) Robust nonlinear position control of BLDC motor with friction, in *2014 IEEE Transportation Electrification Conference and Expo (ITEC)*, Dearborn, Michigan.

12. Lin, H., Yan, W., Wang, J., Yao, Y., and Gao, B. (2009) Robust nonlinear speed control for a brushless DC motor using model reference adaptive backstepping approach, in *2009 International Conference on Mechatronics and Automation*, Changchun, China.

13. Ghandhari, M., Andersson, G., and Hiskens, I. A. (2001) Control Lyapunov Functions for controllable series devices, *IEEE Power Engineering Review*, 21(10), 60–61.

14. Bacciotti, A., and Rosier, L. (2006) *Liapunov Functions and Stability in Control Theory* 2nd ed., 70–77, Springer Science & Business Media, Berlin, Germany.

15. Khalil, H. K. (2001) *Nonlinear Systems* 3rd ed., 116-133, Prentice Hall, Upper Saddle River, New Jersey.

16. MOOG Incorporated, Silencer Series Brushless DC Motors datasheet, *http://www.moog.com/products/motors-servomotors/brushless-motors/inside-rotor-brushless-dc-motors/bn-series/* (accessed July 2015)

17. Brandt, J., Deters, R., Ananda, G., and Selig, M. University of Illinois at Urbana-Champaign, UIUC Propeller Database, *http://m-selig.ae.illinois.edu/props/propDB.html* (accessed July 2015)

ABOUT THE STUDENT AUTHOR

Steven Elliott is currently a student at Southern Methodist University in Dallas, Texas. He plans to earn a Bachelor of Science degree in engineering, followed by graduate school.

PRESS SUMMARY

One area of research and development that has enormous potential for many promising applications is the quadcopter micro-unmanned aerial vehicle (micro-UAV) platform. Quadcopters are poised to become a widely used technology, and improvements in quadcopter controls could have a significant impact on their efficacy. This paper analyzes nonlinear effects on brushless direct current (BLDC) motors when used in quadcopter flying robot applications. Specifically, the goal of this work is to use advanced mathematics to derive a nonlinear closed loop motor control equation and prove the stability of the system using Lyapunov stability analysis. This work includes a custom simulation of the system in MATLAB/Simulink that successfully demonstrates and quantifies the performance of the design.